HEAT TRANSFER AND FRICTION IN A TWO-PHASE BOUNDARY LAYER ON A PLATE

A. M. Grishin and V. I. Zabarin

UDC 532.529

The flow in a two-phase boundary layer under velocity nonequilibrium conditions without heat transfer was examined in [1-3], and in the presence of velocity and temperature nonequilibrium and heat transfer in [4, 5].

Numerical and approximate analytic solutions are obtained in this paper for the problem of a two-phase laminar boundary layer on a plate with a compressible carrying phase under conditions of velocity and temperature nonequilibrium in the presence of heat transfer from the surface in the subsonic flow mode.

1. Formulation of the Problem

We examine the flow of a gas suspension of particles in the boundary layer near a plate installed parallel to the undisturbed stream. We assume that the volume fraction of the chemically inert spherical particles is small, the local flow characteristics differ insignificantly from the mean-volume, the physical density of the particles is much greater than the density of the carrying phase, and the Brownian motion of the particles is not substantial. Then for small Mach numbers the flow of the gas suspension is described by a system of equations in dimensionless form [1, 3]

$$\frac{\partial \rho u}{\partial x}+\frac{\partial \rho v}{\partial y}=0,\quad \frac{\partial}{\partial x}\rho_s u_s+\frac{\partial}{\partial y}(\rho_s v_s)=0,$$
$$\rho\frac{du}{dt}=\frac{\partial}{\partial y}\left(\mu\frac{\partial u}{\partial y}\right)-f_{s,x},\ \rho\frac{dT}{dt}=\frac{\partial}{\partial y}\left(\frac{\mu}{\mathrm{Pr}}\frac{\partial T}{\partial y}\right)-q_s,\ \rho=\frac{1}{T},\tag{1.1}$$
$$\rho_s\frac{d_s u_s}{dt}=f_{s,x},\quad \rho_s\frac{d_s v_s}{dt}=f_{s,y},\quad \rho_s\frac{d_s T_s}{dt}=q_s,$$
$$\frac{d}{dt}\equiv u\frac{\partial}{\partial x}+v\frac{\partial}{\partial y},\ \frac{d_s}{dt}\equiv u_s\frac{\partial}{\partial x}+v_s\frac{\partial}{\partial y}.$$

Here $x = x'/L$, $y = y'/(L\,\mathrm{Re}^{1/2})$ are dimensionless coordinates (the x axis is along the plate while the y axis is along its normal), $u = u'/u'_\infty$, $v = v'(u'_\infty\,\mathrm{Re}^{1/2})$ are dimensionless components of the velocity vector v in the x and y directions, respectively, $\mathrm{Re} = \rho'_\infty u'_\infty L/\mu'_\infty$ is the Reynolds number, L is the characteristic dimension (will be selected later), $\rho = \rho'/\rho'_\infty$, $T = T'/T'_\infty$, $\mu = \mu'/\mu_\infty'$ are the dimensionless density temperature and viscosity coefficient of the gas, $f_s = \rho_s(c_D/c_{D0})(v - v_s)/\sigma_v$, $q_s = \rho_s(c_s/c_p)(\mathrm{Nu}/\mathrm{Nu}_0)\ (T - T_S)/\sigma_T$ are the dimensionless interphasal interaction force and heat flux, $\sigma_v = \tau_v u_\infty/L$, $\sigma_T = 1.5\ \mathrm{Pr}(c_s/c_p)\sigma_v$ are the Stokes number of the dynamic and thermal phase interaction, $\tau_v = \rho_s^0 d_s^2/18\ \mu'$ is the characteristic relaxation time of the particle velocity, $\mathrm{Pr} = \mu' c_p/\lambda$ is the gas phase Prandtl number, d_S, ρ_S^0 are the particle diameter and physical density, c_D and Nu are the coefficients of drag and heat transfer of the particle, $c_{D0} = 24/\mathrm{Re}_S$ and $\mathrm{Nu}_0 = 2$ are values of these coefficients for the Stokes flow mode; $\mathrm{Re}_s = \rho'_\infty|v' - v'_s|d_s/\mu'$ is the particle Reynolds number, c_p, c_S are the gas phase specific heat for constant pressure and the particle specific heat; the subscripts s, ∞ and the prime refer to the particle parameters, to the unperturbed, and to the dimensional parameters.

The boundary and initial conditions have the form

$$u(x,\infty)=1,\ u_s(x,\infty)=1,\ \rho_s(x,\infty)=\rho_{s\infty},\qquad T(x,\infty)=1,\ T_s(x,\infty)=1;\tag{1.2}$$
$$dv_{se}/dx=(v_e-v_{se})/\sigma_{ve};\tag{1.3}$$
$$u(x,0)=0,\ v(x,0)=0,\ T(x,0)=T_w(x);\tag{1.4}$$
$$\rho_s(0,0)=\rho_{s\infty},\ u_s(0,0)=1,\ v_s(0,0)=0,\ T_s(0,0)=1,\tag{1.5}$$

where $T_w(x)$ is a given dimensionless surface temperature and the subscripts w and e correspond to parameters on the plate surface and on the outer boundary of the boundary layer.

Tomsk. Translated from Zhurnal Prikladnoi Mekhaniki i Tekhnicheskoi Fiziki, No. 4, pp. 78-86, July-August, 1988. Original article submitted April 27, 1987.

 0021-8944/88/2904-0528$12.50

The longitudinal velocity component and temperature of the carrying phase in the initial section are determined from self-similar equations in Dorodnitsyn–Lees variables that follow from the system (1.1) as $x \to 0$. The boundary condition (1.3) for the transverse particle velocity component v_s on the outer boundary of the boundary layer reflects the effect of external inviscid flow interaction with the boundary layer in terms of the velocity component v_s. This condition is an additional equation that must be solved in conjunction with the system (1.1) since it contains the function $v(x, y)$ unknown prior to the solution of the problem. Condition (1.3) is obtained from equations [6] for a gas suspension for large Reynolds numbers by the method of merging asymptotic expansions [7].

2. On the Methodology for Numerical Solution of the Problem

It follows from the form of the system (1.1) and the boundary conditions (1.2)-(1.5) that the solution in dimensionless form depends on seven dimensionless parameters $\rho_{s\infty}$, c_s/c_p, σ_{ve}, $\mathrm{Re}_{s\infty}$, T_w, Pr, ω ($\mathrm{Re}_{s\infty} = \rho'_\infty u'_\infty d_s/\mu'$, ω is the exponent in the power-law dependence of the viscosity on the temperature). The first four of these are due to the presence of the dispersed phase. The presence of particles in a gas complicates investigation of the problem (1.1)-(1.5) by known analytic methods substantially especially in the domain of phase velocity and temperature relaxation. Consequently, the solution is found numerically on an electronic computer. The equations for the carrying phase were solved here by the method of [8] with the order of approximation $O(\Delta x^2, \Delta y^4)$ while the equations for the dispersed phase are solved along particle trajectories by the Euler method with corrections having a second order of approximation. Moreover, iterations were performed until the phase values matched with a high degree of accuracy.

The characteristic dimension L along x was selected equal to the length of the particle velocity relaxation on the outer boundary layer boundary $L = \tau_{ve} u'_\infty$ in the computations. A power-law dependence on the temperature with exponent $\omega = 0.645$ is taken for the viscosity coefficient, which corresponds to tabulated data for air with around a 6% error in the 300-2000 K temperature range. The Prandtl number was assumed equal to 0.72. The phase specific heat coefficients were considered constant for simplicity. The drag and heat-transfer coefficients of a single particle were calculated by the approximate dependences [9, 10].

$$c_D = 1 + 1/6(\mathrm{Re}_{s\infty}|u_\infty - u_s|)^{2/3}, \qquad \mathrm{Nu} = 2 + 0.46\,\mathrm{Pr}^{1/3}(\mathrm{Re}_{s\infty}|u - u_s|)^{0.55}. \tag{2.1}$$

3. Discussion of the Results of the Numerical Solution

The structure of the boundary layer for the case of no heat transfer is investigated in [2]. For heat transfer with the surface there are certain features of the velocity profile behavior that are determined by the surface temperature. In the neighborhood of the forward stagnation point in the boundary layer there is a substantial mismatch in the phase velocities and temperatures that diminishes as the coordinate x increases. Two domains can be extracted on the basis of an analysis of the numerical results in the boundary layer: a domain of velocity and temperature relaxation located for $0 \lesssim x \lesssim 2x_s$ (x_s is the particle stopping point on the plate surface); a domain of almost equilibrium flow (in the terminology of [6]), where the longitudinal velocity components and temperatures of the phases are close to each other.

Displayed in Fig. 1 are phase temperature profiles for the cooled plate surface for $T_w = 0.5$, $\rho_{s\infty} = 3$, $c_s/c_p = 1$ in the sections $x = 0$, 0.2, 2, 10 (curves 1-4), the dashes refer to the dispersed phase temperature and the solid lines to the carrying phase temperature. If not especially stipulated, then the particle drag and heat-transfer coefficients are taken Stokesian for simplicity, i.e., $c_D = 1$, $\mathrm{Nu} = 2$. It is convenient to solve the problem (1.1)-(1.5) in Dorodnitsyn–Lees variables x, η, where $\eta = \int_0^y \rho dy/\sqrt{2x}$, since the solution starts with the self-similar according to the conditions of the problem while the limit solution as $x \to \infty$ is also self-similar in these variables. These results from an analysis of Fig. 1 that for $T_w < 1$ when the surface temperature is less than the undisturbed flow temperature, the particles incident in the boundary layer from the undisturbed external flow heat the carrying phase as the coordinate x increases, and are themselves hence cooled. It is interesting to note that deceleration of the particles, and therefore, increase in the density ρ_s of the dispersed phase in the neighborhood of the particle stagnation point x_s result in the most

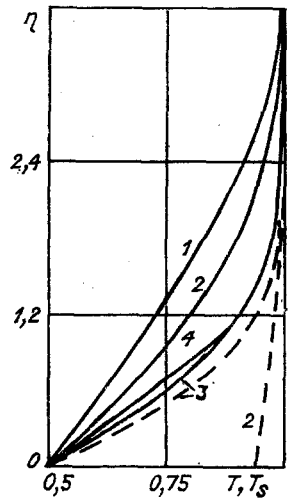

Fig. 1

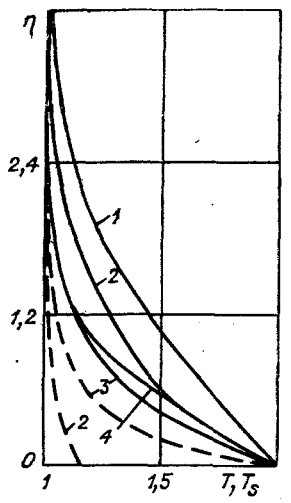

Fig. 2

intensive heat transfer of the phases. Consequently, the temperature of the carrying phase takes on the maximal value in the neighborhood of x_s (the continuous curve 3) for fixed η. As x increases further the difference in the phase temperatures diminishes and the profiles approximate the limit equilibrium solution that corresponds to absence of temperature and velocity slip of the phases (continuous and dashed curve 4 coincide).

For the heated plate surface ($T_w > 1$) on the contrary, the particles incident on the boundary layer cool the carrying phase and are hence themselves heated. Figure 2 shows temperature profiles computed for $T_w = 2$ in the sections x = 0, 0.1, 0.7, 10 (lines 1-4), the remaining parameters are exactly the same as for Fig. 1. It is seen from Fig. 2 that the particle temperature grows monotonically (dashed curves) as the coordinate x increases while the temperature of the carrying phase rises at the beginning for fixed η and then diminishes as x increases. The maximal value of the gas temperature is taken in the neighborhood of x_s for η = const, i.e., in the neighborhood of the most intensive heat transfer of the phases. Relaxation of the temperature profiles (as well as of the velocity profiles) occurs more rapidly in the case of a heated plate surface since the coefficient of interphasal heat transfer is proportional to T^{ω}. The plate surface temperature influences the behavior of the dispersed phase density substantially in the boundary layer.

Displayed in Fig. 3 are profiles of $\rho_{s\infty}/\rho_s$ for a "cold" plate surface $T_w = 0.5$ in the boundary layer sections x = 0, 0.4, 1, 1.6, 3, 10 (curves 1-6, respectively) and analogous profiles in the boundary layer on a "heated" plate surface ($T_w = 2$) in the sections x = 0, 0.2, 0.4, 0.7, 1.4, 8 are shown in Fig. 4. The remaining parameters have the same values as for the previous figures. The density profile has a maximum within the boundary layer (curve 2 in Fig. 3) near the leading edge for the "cold" plate surface because of the influence of the displacing effect of the leading edge boundary layer. This effect predominates over the particle deceleration near the surface on a strongly cooled plate and, consequently, the dispersed phase density near the surface can be less than in the free stream. As x increases further, a profile of the density ρ_s is formed with a maximum on the plate surface (curve 3 in Fig. 3) because of the predominant effect of particle deceleration. Starting with the point $x = x_s$, the density becomes infinite for $\eta = 0$, where, as $\eta \to 0$ $\rho_s \sim O(\eta^{-1})$ (see Sec. 4).

Because of the predominant influence of stagnation over displacement near the heated plate surface the profile of ρ_s has a maximum on the surface. It is interesting to note that as x increases a dispersed phase density profile is formed in the outer part of the boundary layer that is similar to the density profile of the carrying phase which is characteristic for an equilibrium phase flow (see Sec. 5), i.e., for moderate and large η we have $\rho_s > \rho_{s\infty}$ for $T_w < 1$ while $\rho_s < \rho_{s\infty}$ for $T_w > 1$. The stagnation and displacement effects exert a governing influence on the formation of the ρ_s profile near the surface. In this connection, the density profile can have a complex nonmonotonic behavior for a strongly cooled surface.

It is interesting to examine the influence of the surface temperature on the behavior of the heat transmission and friction coefficients on a plate surface. Superposed in Fig. 5 are the heat transmission $c_h Re^{1/2}$ and friction $c_f Re^{1/2}$ coefficients by continuous and dashed lines, respectively, where

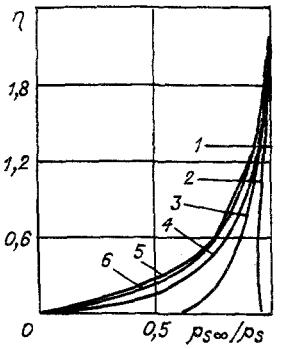

Fig. 3

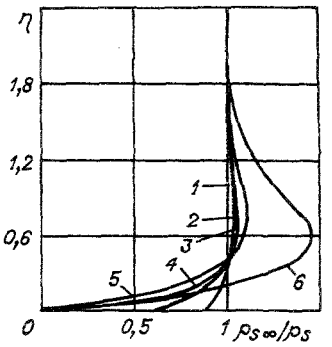

Fig. 4

$$c_h = \frac{\lambda_w \frac{\partial T'}{\partial y'}\Big|_{y'=0}}{\rho'_\infty u'_\infty c_p (T'_\infty - T'_w)}, \quad c_f = \frac{\mu'_w \frac{\partial u'}{\partial y'}\Big|_{y'=0}}{\rho'_\infty u'^2_\infty}.$$

Curves 1-3 correspond to T_w = 0.1, 0.5, and 2, the remaining parameters are the same as for the preceding figures. A remarkable feature of the behavior of c_h, c_f is the presence of the maximum in the neighborhood of the stagnation point x_s of the particles flying along the surface. The reason for this effect is the maximal growth of the mean-integral density ρ_s (over the boundary layer thickness) in the neighborhood of x_s because of particle stagnation. It is seen from the graphs that the initial and limit values as $x \to \infty$ diminish as T_w rises while the maximal values of the coefficients increase, on the contrary. The first effect is well known in boundary layer theory [11] and reflects the influence of the temperature dependence of the viscosity, while the second is apparently caused by two reasons: an increase in the density ρ_s and more intensive heat transfer between the phases. As the surface temperature increases, the maximum of c_h, c_f shifts to the leading edge and the extent of the particle relaxation zone is reduced. For $T_w \geqslant 0.5$ the coordinate x_{max} corresponding to the maximum c_h, c_f approximately equals the coordinate of particle stagnation $x_{max} \approx 0.9/T_w^\omega$ while for a "quite cold" surface ($T_w < 0.5$) $x_{max} \approx 0.5/T_w^\omega$. The Reynolds analogy, valid for single-phase flow on a plate [11]: $c_h = c_f \mathrm{Pr}^{-2/3}$ is satisfied satisfactorily for the curves presented in Fig. 5. Let us note that Eqs. (1.1) do not allow the Crocco integral that is valid in the whole flow domain. The approximate compliance with relationships of the Crocco integral type can only be mentioned for Pr ≈ 0.83, $c_s/c_p \approx 0.8$

$$T_w = T_w + (1 - T_w)u, \quad T_s = T_{sw} + (1 - T_{sw})u_s. \tag{3.1}$$

The influence of actual particle drag and heat transfer laws (2.1) on the friction and heat transfer in the boundary layer is illustrated by the curves 4 in Fig. 5, that correspond to the diminsionless surface temperature T_w = 0.5 and the parameter $\mathrm{Re}_{s\infty}$ = 10. An increase in $\mathrm{Re}_{s\infty}$ corresponds to growth of the particle dimension and the particle velocity (temperature) relaxation time. As $\mathrm{Re}_{s\infty}$ increases (compare with curve 2 obtained for $\mathrm{Re}_{s\infty}$ = 0), more intensive particle stagnation and heat transfer occur, the maximum c_f, c_h shift to the plate leading edge and diminish somewhat.

Presented in Fig. 6 are heat-transmission coefficients for different relationships of the phase specific heats c_s/c_p and dispersed phase densities in the free stream. Curves 1 and 2 correspond to $c_s/c_p = 1/3$ and 3 for T_w = 0.5, and 3 and 4 to analogous c_s/c_p values for a "heated" plate surface (T_w = 2). It is seen that for both a "cold" and "hot" plate surface the heat-transfer coefficient c_h depends on the ratio between the phase specific heats: as the dimensionless specific heat of the particles increases 10 times, the maximum of the heat-exchange coefficient increases approximately two times, the coordinate of the maximum c_h shifts downstream 2.5-2.7 times. Let us note that the heat-exchange coefficient is more responsive to a change in the phase specific heats for the heated plate surface. As a result of computations it turns out that the friction coefficients (meaning the velocity profiles, also) depend weakly on the relations between the phase specific heats (dashed curves 1, 2 and 3, 4 in Fig. 6).

Growth of the disperse phase density in the free stream results in a substantial increase in the heat transfer and friction coefficients. Thus for T_w = 0.5, $\rho_{s\infty}$ = 3, c_s/c_p = 3 (curve 5 in Fig. 6), the maxima of the heat transfer and friction coefficients grow approximately 1.7 times as compared with the case $\rho_{s\infty}$ = 1.

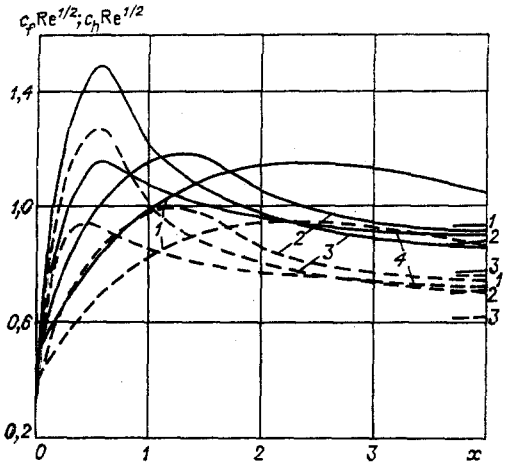

Fig. 5

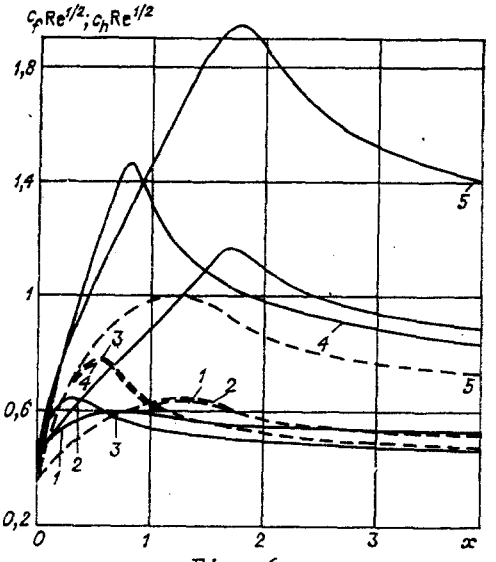

Fig. 6

4. Asymptotic Solution for the Dispersed Phase near the Plate Surface

As characteristic dimension L we select the particle velocity relaxation length on the outer boundary layer boundary. Here and below we consider T_w = const for simplicity. It is later convenient to find the solution in four domains, in each of which the solution possesses characteristic singularities and is represented in simpler form.

Let ε be a small parameter, the distance between the particle trial trajectory and the plate for x = 0. The asymptotic solution for particles of the system of equations (1.1) in domain 1 for $x \sim O(\varepsilon^2)$, $y \sim O(\varepsilon)$ is represented in the form

$$u_s = 1 + O(\varepsilon^2),\ v_s = \varepsilon[v_{s0}(\bar{x}) + O(\varepsilon^2)], \qquad (4.1)$$
$$T_s = 1 + O(\varepsilon^2),\ y_s = \varepsilon + \varepsilon^3 y_{s1}(\bar{x}) + \ldots,\ \bar{x} = x/\varepsilon^2.$$

The solution for the carrying phase in the neighborhood of x = 0 is used essentially to write (4.1). An approximate solution (and even an exact under certain constraints) can be written down for v_{s0}, y_{s1} in (4.1), however the asymptotic behavior of these functions as $\bar{x} \to \infty$ will be of greater interest to us:

$$v_{s0} \sim C,\quad y_{s0} \sim C\bar{x},\ x \to \infty,\quad C = [1 - u_*(1 - T_w)/T_*]/\sigma_{v*},\ C > 0 \qquad (4.2)$$

(u_*, T_*, σ_{v*} are the mean values of the respective functions across the boundary layer). There results from (4.1) that the domain 1 is traversed by the particles parallel to the plate in a first approximation, without altering the longitudinal velocity component and acquiring the transverse velocity component $v_s \sim O(\varepsilon)$ because of the displacing effect of the leading edge boundary layer. The second term for y_s in (4.1) is necessary for merger with the solution in the next domain.

Let us consider the solution in domain 2 for which $x \sim O(1)$, $x < \sigma_{vw} - \varepsilon$, $y \sim O(\varepsilon)$. To the accuracy of the principal terms we have

$$u_s = C_0 - x/\sigma_{vw} + O(\varepsilon),\ v_s = \varepsilon C_1(C_0 - x/\sigma_{vw}) + O(\varepsilon^2),$$
$$T_s = T_w + (1 - T_w)C_0^{-\sigma_{vw}/\sigma_{Tw}}(C_0 - x/\sigma_{vw})^{\sigma_{vw}/\sigma_{Tw}} + O(\varepsilon), \qquad (4.3)$$
$$y_s = \varepsilon(C_2 + C_1 x) + O(\varepsilon^2),\ \rho_s = \rho_{s\infty}/[(1 - x/\sigma_{vw})(1 + C_1 x)] + O(\varepsilon^2).$$

From the merger with the solution of (4.1) and (4.2) in domain 1 the constants C_1, C_2 equal $C_0 = 1$, $C_1 = C$, $C_2 = 1$. We conclude from the form and meaning of the solution (4.3) obtained that the particles in domain 2 near the surface move as in a gas at rest with initial velocities and an initial temperature acquired in the domain 1. The particle trajectories are straight lines deviating from the surface. According to (4.3), the behavior of ρ_{sw} is determined by two factors, the first of which corresponds to the effect of an increase in the density due to particle deceleration while the second, on the other hand, assures a diminution in the density ρ_s because of the displacing action of the leading edge boundary layer. This latter effect is magnified by the "cold" plate according to (4.3). Numerical results

confirm this latter, as presented in Fig. 3 for $T_w = 0.5$ (curve 2). It follows from (4.3) that despite the singularity in the behavior of the density ρ_s as $x \to \sigma_{vw}$ the phase interaction force $f_{s,x}$ remains finite but the interphasal heat flux q_s near the surface grows without limit for $\sigma_{vw} < \sigma_{Tw}$. However, this latter singularity is integrable in y for any $\sigma_{vw}/\sigma_{Tw} > 0$ and, as follows from an analysis of the energy integral equation, does not result in a singularity in the behavior of the heat flux from the gas phase to the surface. For the numerical solution the interphasal heat flux must be integrated with this singularity taken into account.

The domain 3 is in the neighborhood of the particle stagnation point and the condition $|x/\sigma_{vw} - 1| \sim O(\varepsilon)$, $y \sim O(\varepsilon)$ is satisfied for it. The solution in domain 3 has a buffer, i.e., intermediate, structure between the solutions for domains 2 and 4. The main result, needed later, is the solution for the principal term y_s, $y_s \sim \varepsilon C_3$, where $C_3 = C_2 + C_1\sigma_{vw}$ is a constant found from merger with the solution in domain 2.

The last fourth domain lies outside the particle stagnation point. In this domain $x \sim O(1)$, $x > \sigma_{vw} + \varepsilon$, $y \sim O(\varepsilon)$. The solution for the principal terms of the dispersed phase velocity agrees with the solution for the carrying phase

$$u_s = \varepsilon\tau y_{s0}\rho_w/\sqrt{2x} + \ldots, \quad v_{s0} = \varepsilon^2\tau y_{s0}^2\rho_w/2(2x)^{3/2} + \ldots,$$
$$T_s = T_w + \varepsilon q y_{s0}\rho_w/\sqrt{2x} + \ldots, \quad y = \varepsilon y_{s0}(x) + \ldots, \tag{4.4}$$
$$y_{s0}(x) = C_4 x^{1/4}, \quad \rho_s = \varepsilon^{-1}\rho_{s\infty}\sqrt{2x}/(\tau\rho_w y_{s0}^2) + \ldots$$

We obtain $C_4 = C_3\sigma_{vw}^{-1/4}$ from merger with the solution for y_s in domain 3. We conclude from (3.1) that there is a singularity of the type 1/y near the surface in domain 4. However, despite the singularity in ρ_s, it follows from (4.4) that the interphasal interaction force $f_{s,x}$ and the heat flux q_s are quantities on the order of smallness of $O(\varepsilon)$. The viscous terms $O(\varepsilon^{-1})$ in the carrying phase equations (1.1) have the highest order in domain 4, corresponding to the absence of layer influence with $\rho_s \to \infty$ on the solution for the gas phase and the continuous continuation of this latter into domain 4 from the outer domain [for $y \sim O(1)$].

5. Asymptotic Solution for Small Stokes Numbers

Since the Stokes number is a function of the temperature, we shall speak here about the characersitic Stokes number σ, for which we can select $\sigma = \sigma_{vw}$. In this section we consider the characteristic length L independent of σ_v. The case of small Stokes numbers that occurs when the characteristic dimension along x is much greater than the particle velocity relaxation length, is of interest. Let us note that transformation of the variables

$$x_1 = x/\sigma, \quad y_1 = y/\sigma^{1/2}, \quad v_1 = v\sigma^{1/2}, \quad v_{s1} = v_s\sigma^{1/2} \tag{5.1}$$

reduces the boundary layer equation (1.1) to the same equation but with Stokes number one, and without altering the boundary conditions (for $v_w = 0$). Hence, in particular, similarity of the solution in the boundary layer follows from a Stokes number one for large coordinates x and the solution for the small Stokes number with coordinate $x \sim O(1)$ in conformity with (5.1).

From the form of (1.1) with small parameter σ it is convenient to partition the whole flow domain in the boundary layer into three domains: 1) boundary layer for $x \sim O(\sigma)$; 2) boundary layer for $x \sim O(1)$, $y \sim O(1)$, the particles in domain 2 are incident from the undisturbed flow domain; 3) the sublayer for $x \sim O(1)$, $y \sim \varphi(\sigma)$, $\lim_{\sigma\to 0}\varphi(\sigma) \to \infty$ [$\varphi(\sigma)$ must be determined], where the particles in domain 3 are incident from domain 1.

Let us examine the solution in domain 1. The transformation of variables (5.1) reduces (1.1) to the same equation but with Stokes number one. The equations are not simplified, their solution must be obtained numerically. Substantial phase interaction occurs in domain 1, resulting in phase velocity and temperature relaxation to certain limit solutions which are then transferred into domain 3. The orders of the variables are determined from (5.1). One of the singularities in the solution in domain 1 is an inhomogeneous dispersed phase profile even for $T_w = 1$ [2].

Furthermore, let us examine (1.1) in domain 2. It is easy to obtain that there is no phase velocity and temperature slip in a first approximation as $\sigma \to 0$ and the solution will satisfy the "effective" gas flow conditions with an increased constant density $(1 + \rho_{s\infty})$.

Since the characteristic dimension along x is missing in this domain, the solution is then found from the self-similar problem

$$\frac{\partial}{\partial\eta_\Sigma}(lu_{\eta\Sigma}) + f_\Sigma u_{\eta\Sigma} = 0,\ \frac{\partial}{\partial\eta_\Sigma}\left(\frac{l}{\mathrm{Pr}_\Sigma}T_{\eta\Sigma}\right) + f_\Sigma T_{\eta\Sigma} = 0,\ \rho_s/\rho = \rho_{s\infty}. \tag{5.2}$$

Here $\eta_\Sigma = \sqrt{1+\rho_{s\infty}}\,\eta$; $f_\Sigma = \int_0^{\eta_\Sigma} u\,d\eta$; $\mathrm{Pr}_\Sigma = \mathrm{Pr}(1+\rho_{s\infty}c_s/c_p)/(1+\rho_{s\infty})$; $l = \mu\rho/\mu_e\rho_e$. The boundary conditions for the system (5.2) remain (1.2) and (1.4) as before as follows from the procedure for merger with the solution in domain 3. Let us note that the structure of the solution in domains 2 and 3 is such that the presence of the thin sublayer 3 does not disturb the solution for the velocity and temperature in domain 2. Consequently, the friction and heat flux at the wall are found from (5.2). The system (5.2) is well known in boundary layer theory [11] and describes the solution of the compressible boundary layer equations on a plate. The effective Prandtl number can vary substantially depending on Pr, $\rho_{s,\infty}$, and c_s/c_p. Particularly for $c_s = c_p$, it follows from (5.2) that $\mathrm{Pr}_\Sigma = \mathrm{Pr}$ and then the limit solution is obtained for $\sigma \to 0$ from the solution of the initial problem (1.1)-(1.5) at the forward stagnation point by transformation of the coordinate $\eta \to \eta_\Sigma$. The heat transmission and friction coefficients of the limit solution are here expressed in the form

$$c_h = \sqrt{1+\rho_{s\infty}}c_{h0},\ c_f = \sqrt{1+\rho_{s\infty}}c_{f0}, \tag{5.3}$$

where c_{h0}, c_{j0} are heat transmission and friction coefficients for x = 0.

The necessity to introduce the sublayer 3 occurs in connection with the formation of a thin domain with substantially inhomogeneous density ρ_s near the surface. As in domain 2, there is no phase velocity and temperature slip in a first approximation in 3. The velocity and temperature are determined by expanding the solution of (5.2) for small y. But the equation for the dispersed phase density is $\mathbf{v}\cdot\mathrm{grad}\,\rho_s = 0$. In domain 3 (small y coordinates) we obtain from this equation that ρ_s is conserved along the particle trajectory

$$y_s = \theta(x\sigma)^{1/4}. \tag{5.4}$$

The order of the coordinate y_s in (5.4) is determined from the condition for merger with the solution in domain 1, where θ is the merger constant. For $T_w = 1$ analogous results follow from the data of this section [2]. Asymptotic solutions (5.3) for the friction and heat-transmission coefficients are superposed in Fig. 1 by dashed curves. It is seen for the curves 6 (large x coordinate of small Stokes number) in Figs. 2 and 3 that with the exception of a thin domain near the surface, the density profiles ρ_s are similar to the 1/T profiles according to (5.2).

The asymptotic solutions obtained confirm and supplement the numerical results.

LITERATURE CITED

1. V. P. Stulov, "On laminar boundary layer equations in a two-phase medium," Izv. Akad. Nauk SSSR, Mekh. Zhidk. Gaza, No. 1 (1979).
2. A. N. Osiptsov, "On the structure of the laminar boundary layer of a dispersed mixture on a flat plate," Izv. Akad. Nauk SSSR, Mekh. Zhidk. Gaza, No. 4 (1980).
3. M. E. Deich and G. A. Filippov, Gasdynamics of Two-Phase Media [in Russian], Energoizdat, Moscow (1981).
4. A. N. Osiptsov, "Boundary layer on a blunt body in a dusty gas flow," Izv. Akad. Nauk SSSR, Mekh. Zhidk. Gaza, No. 5 (1985).
5. S. V. Peigin, "Hypersonic spatial viscous shock layer in a two-phase flow," Prikl. Mat. Mekh., No. 2 (1984).
6. F. Marble, "Dynamics of dusty gases," Mekhanika [Russian translation], No. 6 (1971).
7. J. Cole, Perturbation Methods in Applied Mathematics [Russian translation], Mir, Moscow (1972).
8. I. V. Petukhov, "Numerical analysis of two-dimensional flows in the boundary layer," Numerical Methods of Solving Differential and Integral Equations and Quadrature Formulas [in Russian], Nauka, Moscow (1964).
9. V. M. Voloshchuk, Introduction in the Hydrodynamics of Coarsely Dispersed Aerosols [in Russian], Gidrometeoizdat, Leningrad (1971).
10. R. I. Nigmatulin, Principles of the Mechanics of Heterogeneous Media [in Russian], Nauka, Moscow (1974).
11. H. Schlichting, Boundary-Layer Theory, 6th Ed., McGraw-Hill (1968).